Two-Phase Flow and Heat Transfer in Pin-Fin Enhanced Micro-Gaps

Steven A. Isaacs, Yoon Jo Kim, Andrew J. McNamara, Yogendra Joshi, Yue Zhang, Muhannad S. Bakir
Georgia Institute of Technology
Atlanta, Georgia, 30332
Email: sisaacs3@gatech.edu

ABSTRACT

Thermal management of integrated circuits (IC) has emerged as one of the key challenges for continued performance enhancement of modern microprocessors. Cooling schemes utilizing two-phase, microfluidic technologies are some of the more promising modular thermal management solutions for next generation devices. In this study, the flow and heat transfer in pin-fin enhanced micro-gaps are experimentally investigated. It has been known that pin-fin structures inside micro-gaps can increase convective heat transfer coefficients in single phase flow conditions. However, two-phase microfluidic cooling is becoming an increasingly popular method in thermal control of electronics, and this cooling strategy has not been well characterized for pin-fin enhanced micro-gaps. Pin-fin, micro-gap structures studied had a pin diameter, height and pitch of 150μm, 200μm and 225μm, respectively, providing an aspect ratio of 1.33. Both the overall micro-gap width and length are 1cm. The working fluid used was R245fa. The structure contained a transparent cover which allowed for visualization of flow through the micro-gap. A high speed camera allowed for image capture and characterization of various two-phase flow regimes. The thermal performances of the heat sink were experimentally evaluated using pressure drop and temperature measurements.

KEY WORDS: two phase, pin fin, heat sink, liquid cooling, micro-gap

NOMENCLATURE

A	area (m^2)
c	temperature coefficient
D	fin diameter (m)
h	heat transfer coefficient (W/m^2K)
k	fin thermal conductivity (W/mK)
L	length (m)
M	fraction
$\dot{m}$	mass flowrate (kg/s)
N	number of fins
P	fin perimeter (m)
q	heat load (W)
R_e	Electrical resistance (Ω)
R_o	Reference heater resistance (Ω)
S	pitch (m)
T	temperature (K)

Greek symbols

α	average heat transfer coefficient ($W/m^2 K$)
η	fin efficiency
Δ	change in

Subscripts

b	base
b_exp	base exposed
eff	effective
f	fin
f_corr	fin corrected
f_cross	fin cross-section
f_exp	fin exposed
g	vapor
in	inlet
o	reference value
out	outlet
∞	fluid reference

INTRODUCTION

As today's electronics advance in functionality, the need for high heat dissipation has become a popular topic. As can be seen from various studies on the progression of IC cooling, air-cooling methods are reaching their limits, as chip heat dissipation requirements rise [1][2]. While these studies indicate air-cooling limits well below 100 W/cm^2, next generation chips are expected to reach a required heat load significantly greater than 100 W/cm^2. Extensive studies involving single phase liquid cooling using water have shown vast improvements compared to air cooling in configurations such as microchannels and microgaps, which can be further enhanced through augmentation features such as micro pin fins [3][4]. Despite its superior heat transfer performance, water has inherent disadvantages when used for electronic cooling, including possible shorting in the case of leakage and erosion. One answer to these issues has been the implementation of low pressure refrigerants, allowing the capability to achieve saturation temperatures closer to chip temperatures. Recent micro channel studies have indicated that low pressure, two-phase refrigerant systems can dissipate heat loads as high as 350 W/cm^2 [5].

This paper presents two-phase heat transfer performance and flow visualizations over an enhanced micro gap with a staggered pin fin configuration for multiple heat loads ($20W/cm^2$ – $35W/cm^2$) and flowrates (20ml/min – 40ml/min), utilizing R245fa as the working fluid. Heat transfer coefficients for each case are presented and qualitative observations were made. Also, flow characteristics for each sample were recognized by flow visualization and flow regimes were defined.

EXPERIMENTAL SETUP

The experimental platform used in this study consisted of a cleanroom fabricated, silicon, pin fin sample and a closed, flow loop.

Pin Fin Sample

The micro pin fin sample had etched, silicon, cylindrical fins and was fabricated in-house using cleanroom facilities. The extended surfaces were populated on a 1cm x 1cm square surface that included inlet and outlet flow passages. The height, pitch and diameter of the pins were 200µm, 225µm, and 150µm, respectively (Figure 1). The pins were located in 43 rows with 42 pins per row. In order to simulate uniform microprocessor heating, a Pt heater, in a spiral pattern, was built into the sample directly behind the pin fin surface.

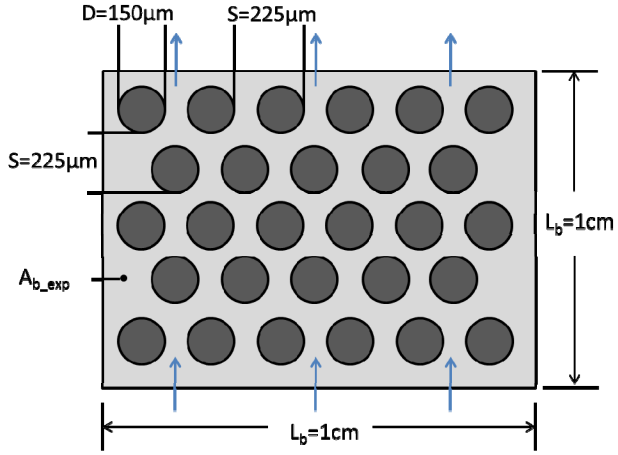

Fig. 1 Schematic of pin fin layout and dimensions

A solid, clear cover was bonded to the top of the pins. This had two main purposes. The first was to completely seal the pins and flow passages. The second was to provide a means of visualizing flow through the sample during live experimental runs. Inlet/Outlet ports mounted on the back of the sample corresponding to the inlet and outlet passages allowed for connections to the refrigerant flow loop (Figure 2).

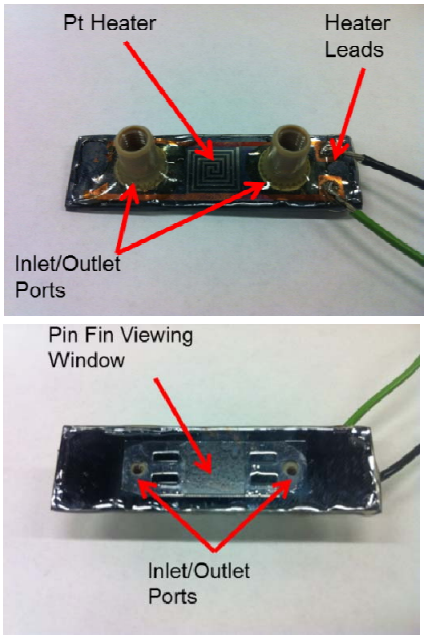

Figure 2. Image of sample with inlet/outlet ports, Pt heater, and leads

Table 1. Experimental Uncertainties

Quantity	**± Uncertainty**
I/O temperature, T (°C)	0.5 °C
I/O pressure (kPa)	0.25% FS
Mass flux, G (kg/m^{2}s)	3%
Current, I (amps)	0.2%
Voltage, V (volts)	0.2%
Fin height	3%
Sample length, L (cm)	2%
Sample width, w (cm)	2%
Heat transfer coefficient, h (W/m^{2}K	14-18%

Closed Flow Loop

The refrigerant flow loop constructed to test the temperature and pressure drop across the uniform heated pin fin sample can be seen in Figure 3. This setup consists of a primary refrigerant loop and secondary cooling loop. The primary loop is composed of a pump, flowmeter, two heat exchangers, metering valve and a pre-heater connected with insulated ¼" copper tubing. The secondary loop simply supplies chilled water to the backside of the copper heat exchangers. A Cole-Palmer digital magnetic gear pump and a McMillan microturbine flowmeter with a 20 to 200 ml/min measurement range were used. The copper heat exchangers assisted in heat removal downstream of the pin fin sample and before the pre-heater. The pre-heater and metering valve were located directly upstream of the pin fin sample and allowed for temperature and pressure control based on the degree of prescribed subcooling. Swagelok brass inline 15 micron-sized element pores provided means of filtering the working fluid. Pressure and temperature measurements were taken at the inlet and outlet of the pin fin sample to measure the sample's thermal performance. Uncertainties associated with the pressure transducers and T-type thermocouples were 0.25% FS and 0.5°C. Table 1 shows uncertainties of experimental measurements. Propagation of uncertainty analysis was used to determine uncertainty of calculated results.

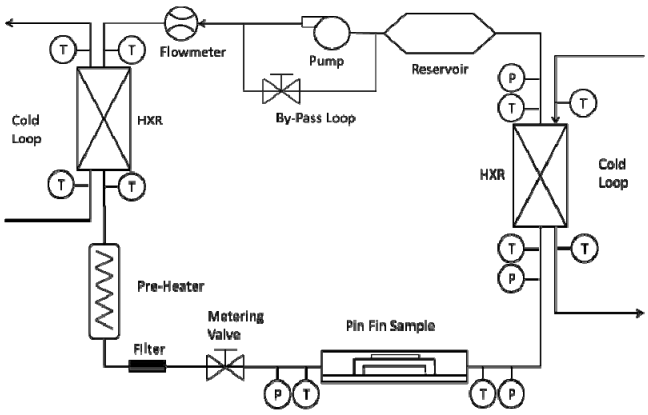

Fig 3. Schematic of closed refrigerant flow loop.

The pin fin sample was connected to the refrigerant loop via clear vinyl tubing. Insulation was wrapped around the sample and clear tubing. Small sections of the tubing directly before and after the inlet/outlet ports were exposed to serve as viewing windows of the flow before and after the pin fin sample.

With the sample facing down on the acrylic, a mirror was placed under the stand at a 45° angle. A Photron high speed camera set at 100 fps was then set up to record video of flow experiments.

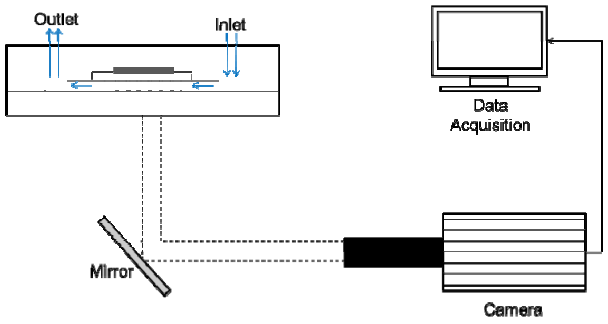

Fig. 5 Diagram of flow visualization setup

EXPERIMENTAL PROCEDURE

To begin the experimental runs, the system pump was used to run refrigerant R245fa through the primary loop and chilled water was run through the secondary loop side of the heat exchangers. The metering valve and pre-heater located directly upstream of the pin fin sample allowed for inlet pressure and temperature control. Subcooling was kept between 15 and 20 °C for this study. With flowrate and heat flux under control, sample inlet pressure ranged from 183 to 230 kPa. Pressure drop across the sample ranged from 33kPa for 20W/cm^2 heat flux to 67 kPa for 35W/cm^2 heat flux. The system was allowed to set until steady state conditions were reached. To initiate boiling, the flowrate was reduced to a small reading. The heater power was gradually raised in small increments until flow boiling could be seen (~20W/cm^2). After this, the flowrate and heater power were set to values corresponding to desired test values.

For this study, twenty different cases were run at various heater powers and flowrates. Power levels ranged from 20 to 35W. The flowrates ranged from 20 to 40 ml/min. The inlet port viewing window was monitored to ensure a subcooling inlet condition was maintained. For each case, the system was allowed to reach a steady state condition which took roughly 5 minutes. Once steady state was reached, data was collected at 1Hz. An average was obtained over these data points to get final measured values. Video of flow boiling over the sample was taken. Data was collected and used in the following reduction.

DATA REDUCTION

With a certain specific heat c_p, the refrigerant entered the sample at the inlet port. The power into the flowing refrigerant, q_{eff}, was calculated from

$$q_{eff} = q_{total} - q_{loss} \quad (1)$$

where the heat loss, q_{loss}, was calculated from single phase experiments. At a power of 12W, an 8% heat loss through the sample was found using a basic energy balance. This was the highest power range for single phase measurements based on the structural integrity of the pin-fin sample so this "rough" heat loss estimate was used throughout the two-phase calculations and reflected in uncertainty estimation.

For each case, an average heat transfer coefficient, h, was calculated using the fin efficiency model [6]. This model utilized the adiabatic fin tip condition with a corresponding corrected length. From here, an iterative approach was used to obtain the average heat transfer coefficient for each case shown by the diagram in Figure 6.

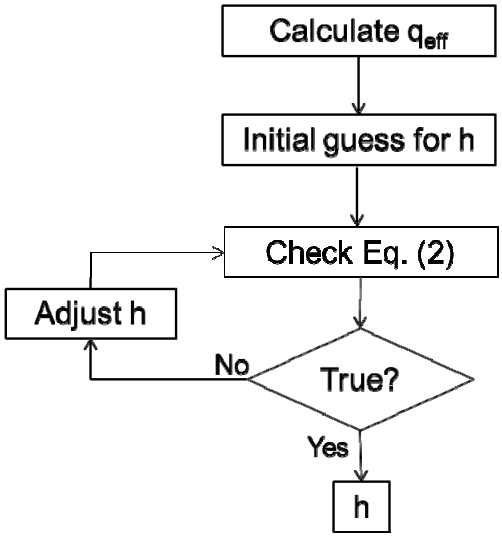

Figure 6. Flow diagram of iterative procedure for heat transfer coefficient calculation

The effective power into the fluid stream can then be expressed as

$$q_{eff} = \alpha(A_{b\_exp} + \eta A_{f\_exp})(T_w - T_\infty) \quad (2)$$

where T_∞ was the temperature of the fluid flowing over the fin array, i.e, the saturation temperature of the refrigerant at the corresponding pressure over the sample. With the focus of this study on basic thermal performance of the enhanced micro-gap and to compliment the average wall temperature measurement, a simplified approach was used to calculate an average saturation temperature over the array [8]. An average pressure drop between inlet and outlet measurements was calculated and was used to estimate average fluid saturation temperature across the array. Average saturation temperature ranged between 29.8°C at 166 kPa and 34.4 °C at 196 kPa. The pressure drop through the clear tubing of the sample was assumed to be negligible compared to the pressure drop across the pin fins. The pressure measurement uncertainty resulted in an uncertainty in saturation temperature of < 2%.

Taking advantage of the linearity of the Pt heater, the heater was used for estimating the temperature at the base of the pin fins using the temperature coefficient equation

$$R(T) = R_o(1 + c\Delta T) \quad (3)$$

where R is the heater resistance. R_o is the reference heater resistance measured at ambient temperature. The temperature coefficient, c, had a value of 3.327e-3 for this study.

For quality calculations, the following process was used (h represents enthalpy for equations 4 and 5).

$$q_{eff} = \dot{m}(h_{out} - h_{in}) \quad (12)$$

where h was the inlet/outlet enthalpy of the working medium corresponding to inlet/out pressure measurements according to R245fa property data. Since the inlet was maintained subcooled, h_{in} was calculated as the fluid enthalpy entering the sample. Vapor quality at the outlet of the sample was then determined by

$$x = (h_{out} - h_{f_{out}}) \,/\, (h_{g_{out}} - h_{f_{out}}) \quad (13)$$

RESULTS

A few interesting trends can be seen from Figures 7 and 8. As heat flux is increased, the average heat transfer coefficient decreases. Also, the average heat transfer coefficient decreases with increasing vapor quality. This result was unexpected with the anticipation that heat transfer coefficient would improve with a larger amount of flow boiling. Studies with flow boiling through microchannels indicate this deceasing trend, though at very high heat fluxes [7][8]. At low heat fluxes, however, heat transfer coefficients increased with increasing heat fluxes. A similar situation is identified with pin fin studies [9]. It was shown that once the heat transfer coefficient hit a maximum it began to decrease for increasing heat fluxes. With no supporting evidence of decreasing heat transfer coefficient before a maximum, it is believed the range of the current study falls after a maximum value that could not be shown with the current experiment..

Previous studies have identified nucleate boiling and convective boiling as dominate heat transfer mechanisms in pin fin arrays [4][9].Nucleate boiling is characterized by bubbly flow. In this region, vapor bubbles grow and detach from the heated surface. The other regime is convective boiling which is characterized by annular flow with a liquid film separating the solid surface and vapor volume.

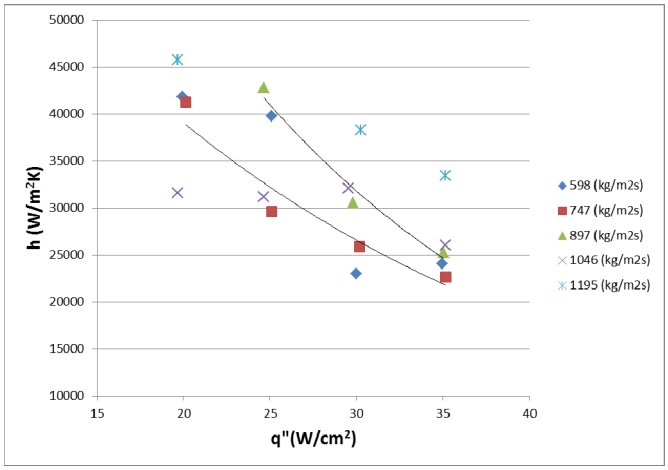

Figure 7. Average heat transfer coefficient vs. effective heat flux for different flowrates

From Figure 9 and 10, two separate sections, liquid and liquid+vapor, are apparent on the samples. In order to get a better understanding of the vapor quality during the experiments, Table 2 displays these values for each case. Vapor quality tends to increase for increasing heat loads and decrease for increasing flowrates. Also, the images in Figures 9 and 10 help illustrate these vapor quality trends. The nucleation begins towards the middle of the pin fin array for high heat loads and low flowrates, with large, triangle-shaped liquid+vapor wakes covering a large portion of the rear of the array (high vapor quality). For increasing flowrates and decreasing heat loads these nucleation points migrate towards the back of the sample. The two-phase front also moves as the wakes behind these nucleation points decreases in size (decreasing vapor quality). A similar boiling region movement, which involves upstream expansion with increasing heat flux, has been apparent in literature [9]. The migration of the two-phase front had a much stronger dependence on heat flux then it did with flowrate. (See Figure 9 for effect of flowrate images). This interesting wake structure demonstrates the two-dimensional spreading of vapor bubbles around the pin fins and suggests that pin fin enhancement also provides a flow distribution advantage when compared to microchannel, two-phase flow. We posit that the triangular features of the vapor wakes are attributed to the inherent 2D geometry of the pin fin micro-gap, allowing for lateral pressure distribution and vapor spreading behind nucleation points. Similar trends were observed for all experimental runs.

Table. 2 Outlet vapor quality, x, at test flowrates and heat fluxes

	20W/cm^2	25W/cm^2	30W/cm^2	35W/cm^2
598kg/m^{2}s	0.259	0.329	0.409	0.473
747kg/m^{2}s	0.224	0.284	0.347	0.414
897kg/m^{2}s	0.194	0.245	0.291	0.347
1046kg/m^{2}s	0.167	0.218	0.260	0.314
1195kg/m^{2}s	0.153	0.199	0.243	0.282

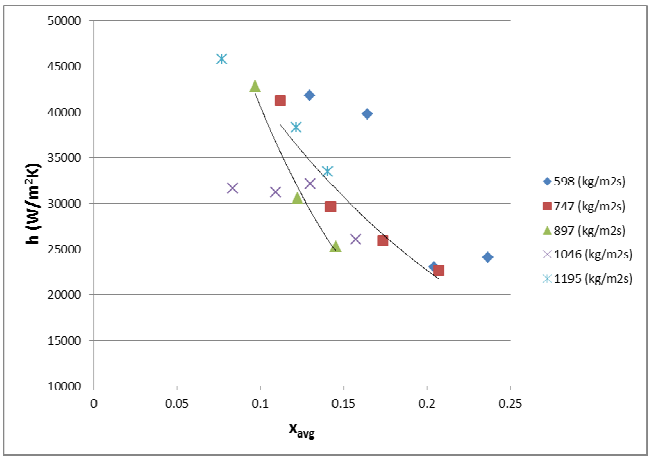

Figure 8. Average heat transfer coefficient vs. quality

In order to explain the heat transfer coefficient characteristics observed during the study, dominant heat transfer mechanisms for each type of internal, flow boiling regime were considered. For the single-phase region, heat would be transferred by convection from the sample base and pin fins to the liquid. For nucleate boiling, heat transfer is dominated by continuous wetting of the surface by liquid for bubbly flow while heat transfer to vapor occurs when bubbles coalesce. Annular flow begins as a liquid film covering the pin fins and base but eventually forms dry areas (dry-out) as heat flux is increased. These dry areas constitute a drop in heat transfer coefficient since the thermal conductivity of vapor is significantly less than liquid. Moreover, Qu and Siu-Ho [4] identified annular flow as the dominant flow regime in pin fin enhanced gaps with liquid film covering the pin fin surfaces. This film was sustained by a balance between deposition of

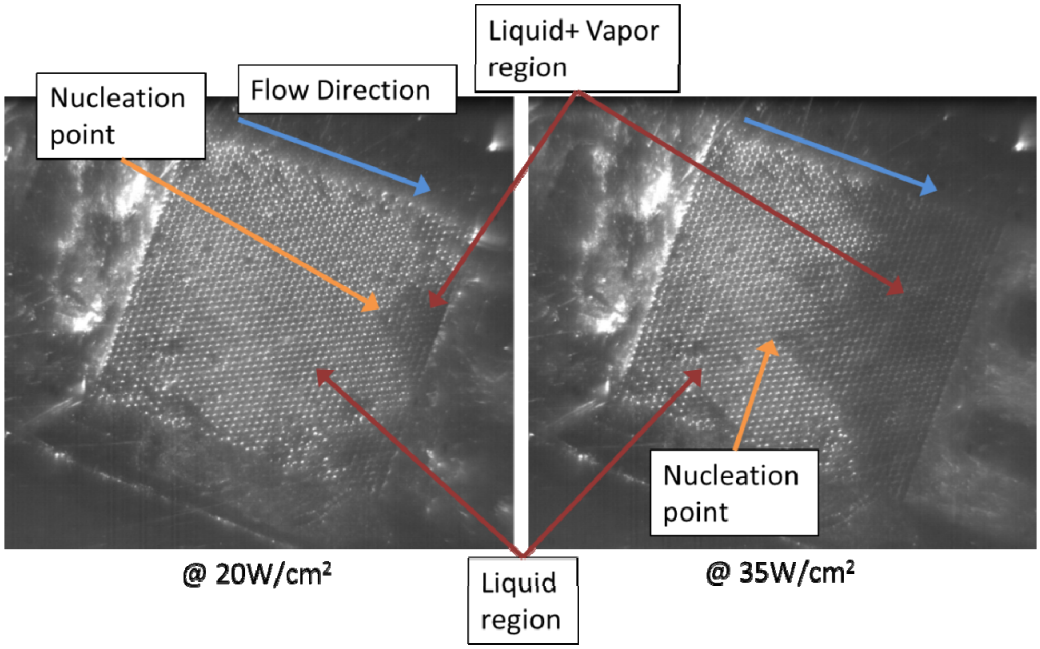

Figure 9. Two-phase flow visualization of the pin fin sample at 1046 kg/m^{2}s

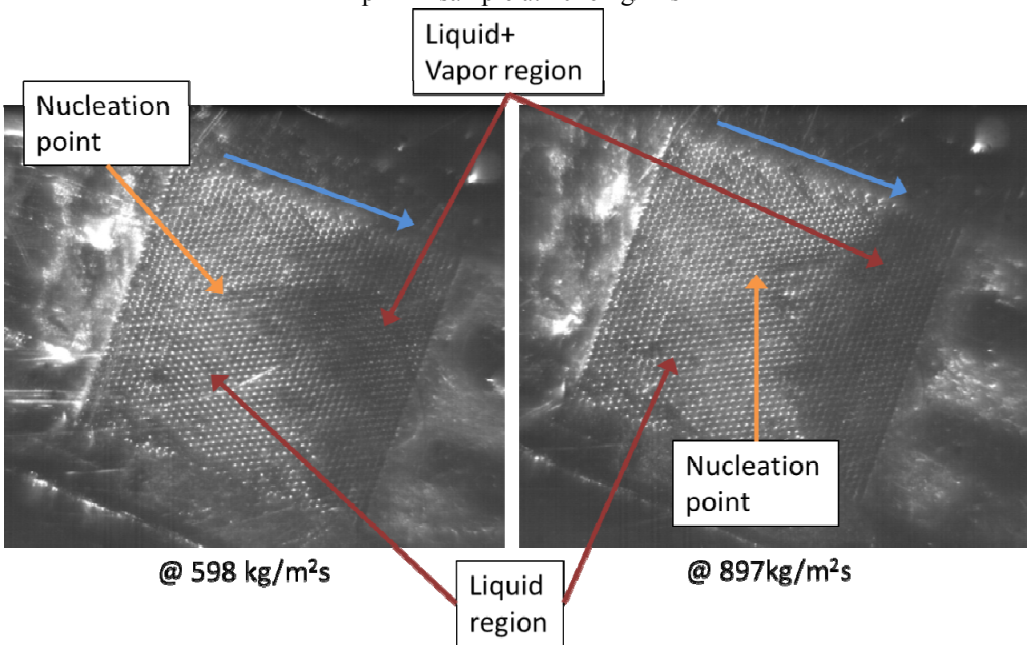

(a)

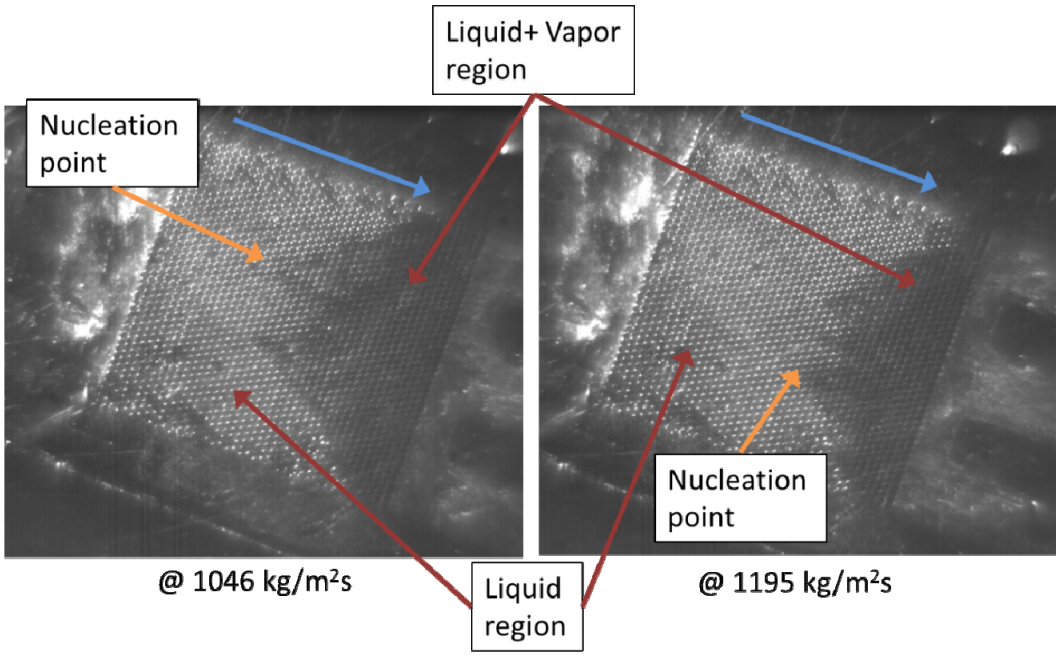

(b)

Figure 10. Flow images at heater power of 30W at a) 598 and 897 kg/m^{2}s and b) 1046 and 1195 kg/m^{2}s

discrete liquid droplets and evaporation.

For the current study, one can develop a reasonable explanation for the heat transfer trends. For high flowrates and low heat fluxes the flow map shows small triangle-shaped vapor wakes towards the end of the sample (top image in Figure 9). When the heat flux is increased the vapor wakes increase in size, thus increasing vapor quality and covering a larger area of the pin fin sample. The fact that heat transfer coefficient values drop coincides with an assumption that the majority of liquid+vapor region is not experiencing nucleate boiling and, instead, is dominated by partial and intermittent dry-out where heat transfer coefficients are known to decrease.

CONCLUSION

In this study, a micro scale, pin fin enhanced gap was shown to have interesting flow boiling characteristics using R245fa. Trends in the heat transfer coefficients were clearly stated and explained according to established flow boiling regimes. Of course, the validity of these regimes are open to question since they are classically used for larger scale setups. In comparison to supporting literature, heat transfer coefficient results indicate a possible early transition to post-CHF trends. From flow visualizations unique, two-dimensional, triangular-shaped vapor wakes were shown to form downstream of nucleation points. These structures were attributed to two-dimensional spreading over the array, an advantage of pin fin enhanced micro-gaps. Also, the location of nucleation points across the array had a strong dependence on heat flux and mild dependence on liquid flowrate. With these observations and a review of possible flow boiling regimes, it was determined the two-phase region of the array was dominated by partial and intermittent dry-out.

ACKNOWLEGMENTS

We would like to acknowledge support from the Department of Defense.

References

[1] M. Saini and R. L. Webb, “Heat Rejection Limits of Air Cooled Plane Fin Heat Sinks for Computer Cooling,” IEEE Transactions on Components and Packaging Technologies, vol. 26, no. 1, pp. 71-79, March. 2003.

[2] M. J. Ellsworth, R. E. Simons,”High Powered Chip Cooling-Air and Beyond”, *Electronics Cooling*, Aug. 2005, http://www.electronics-cooling.com/.

[3] P. S. Lee and S. V. Garimella, “Saturated Flow Boiling Heat Transfer and Pressure Drop in Silicon Microchannel Arrays,” Int. J. Heat and Mass Transfer, 51:789-806, 2008

[4] W. Qu and A. Siu-Ho, “Experimental Study of Saturated Flow Boiling Heat Transfer in an Array of Staggered Micro-pin-fins,” Int. J. Heat and Mass Transfer, 52:1853-1863, 2009

[5] J. E. Park and J. R. Thome,”Critical Heat Flux In Multi-Mircochannel Copper Elements With Low Pressure Refrigerants,” Int. J. Heat and Mass Transfer, 53:110-122, 2010

[6] F. P. Incopera and D. P. Dewitt, “Fundamentals of Heat and Mass Transfer,” 6th edition. Wiley, 2007

[7] B. Agostini, J. R. Thome, M. Fabbri, B. Michel, D. Calmi, U. Kloter, “High Heat Flux Flow Boiling in Silicon Multi-microchannels – Part I: Heat Transfer Characteristics of Refrigerant R236fa,” Int. J. Heat and Mass Transfer, 51:5400-5414, 2008

[8] B. Agostini, J. R. Thome, M. Fabbri, B. Michel, D. Calmi, U. Kloter, “High Heat Flux Flow Boiling in Silicon Multi-microchannels – Part II: Heat Transfer Characteristics of Refrigerant R245fa,” Int. J. Heat and Mass Transfer, 51: 5414-5425, 2008

[9] A. Kosar, Y. Peles, “Boiling Heat Transfer in a Hydrofoil-based Micro Pin Fin Heat Sink,” Int. J. Heat and Mass Transfer, 50: 1018-1034, 2007